CZECH TECHNICAL UNIVERSITY
IN PRAGUE

FACULTY OF ELECTRICAL ENGINEERING

Effect of swept-sine speed on distortion-product otoacoustic emissions

Bachelor Thesis

2024 Ruoting Wang

Ing. Václav Vencovský, Ph.D.

BACHELOR'S THESIS ASSIGNMENT

I. Personal and study details

Student's name: **Wang Ruoting** Personal ID number: **490855**

Faculty / Institute: **Faculty of Electrical Engineering**

Department / Institute: **Department of Electrical Power Engineering**

Study program: **Electrical Engineering and Computer Science**

II. Bachelor's thesis details

Bachelor's thesis title in English:

Effect of swept-sine speed on distortion-product otoacoustic emissions

Bachelor's thesis title in Czech:

Vliv rychlosti rozmítání tónu na distorzní produkt otoakustických emisí

Guidelines:

Distortion-product otoacoustic emissions (DPOAEs) are sound signals generated due to nonlinear distortion in the inner ear. These sounds are evoked with two tones presented into the ear and can propagate back into the middle ear and outer ear, where they can be recorded with a microphone. Swept sines have been used for almost two decades to evoke DPOAEs because they offer a fast and reliable measurement method. Because DPOAEs are weak signals with intensities close to the intensity of background noise, evoking stimuli must be presented repeatedly in order to suppress background noise by averaging. This thesis is focused on finding the optimal speed for the measurement technique using synchronized swept sines. To achieve the thesis aim, a computational model of the cochlea and DPOAEs recorded in human participants will be used.

Bibliography / sources:

[1] A. Novak, P. Lotton, and L. Simon, "Synchronized Swept-Sine: Theory, Application, and Implementation," J. Audio Eng. Soc., vol. 63, no. 10, pp. 786-798, (2015 October.). doi: https://doi.org/10.17743/jaes.2015.0071

Name and workplace of bachelor's thesis supervisor:

Ing. Václav Vencovský, Ph.D. Department of Radioelectronics FEE

Name and workplace of second bachelor's thesis supervisor or consultant:

Date of bachelor's thesis assignment: **01.03.2023** Deadline for bachelor thesis submission: **26.05.2023**

Assignment valid until: **16.02.2025**

Ing. Václav Vencovský, Ph.D.	doc. Ing. Zdeněk Müller, Ph.D.	prof. Mgr. Petr Páta, Ph.D.
Supervisor's signature	Head of department's signature	Dean's signature

III. Assignment receipt

The student acknowledges that the bachelor's thesis is an individual work. The student must produce his thesis without the assistance of others, with the exception of provided consultations. Within the bachelor's thesis, the author must state the names of consultants and include a list of references.

Date of assignment receipt

Student's signature

© ČVUT v Praze, Design: ČVUT v Praze, VIC

Topic registration form

Declaration

I hereby declare that this bachelor's thesis is the product of my own independent work and that I have clearly stated all information sources used in the thesis according to Methodological Instruction No. 1/2009 – "On maintaining ethical principles when working on a university final project, CTU in Prague

Date signature

Acknowledgments

We would like to thank two anonymous reviewers for their helpful comments on the manuscript. This work was supported by the project 23-07621J of the Czech Science Foundation (GACR).

List of contents

List of abbreviations

OAE——Otoacoustic emissions

SOAE——Spontaneous otoacoustic emissions

EOAE——Evoked otoacoustic emissions

DPOAE——Distortion product otoacoustic emissions

PySide2——a Python module that provides bindings for the Qt application framework

SSS——Synchronized Swept-Sine

RMS——Root mean square

dB——Conversion to Decibels

NF——The noise floor

Abstract

DPOAEs (Distortion product otoacoustic emissions) are sounds generated in the inner ear because of nonlinear distortion. They can be recorded in the outer ear using a microphone, with swept sines being a common method for measurement for nearly two decades. This bachelor's thesis provides a comprehensive investigation into the effect of swept-sine speed on DPOAEs, utilizing the novel Synchronized Swept-Sine methodology. It also examines the use of PySide2 in creating an interactive user interface specifically for DPOAE measurements. The thesis conducts controlled experiments to understand the nuanced impact of varying the speed of swept sines on DPOAE measurements. The findings indicate that the DP-gram, remains roughly consistent across four different frequency sweep rates, as demonstrated through experimental data.
Key words: Distortion product otoacoustic emissions, PySide2, Synchronized Swept-Sine, The noise floor, Signal analysis.

Abstrakt

DPOAE jsou zvuky generované ve vnitřním uchu v důsledku nelineárního zkreslení. Lze je zaznamenat ve vnějším uchu pomocí mikrofonu, přičemž rozmítané tony jsou běžnou metodou měření po téměř dvě desetiletí. Tato bakalářská práce poskytuje komplexní výzkum vlivu rychlosti rozmítání tonu na DPOAE s využitím nové metodologie Synchronized Swept-Sine. Zkoumá také použití PySide2 při vytváření interaktivního uživatelského rozhraní speciálně pro měření DPOAE. Práce provádí experimenty, aby porozuměla vlivu měnící se rychlosti rozmítaných tonů na měření DPOAE. Zjištění naznačují, že DP-gram,, zůstává zhruba konzistentní napříč čtyřmi různými frekvencemi rozmítání, jak bylo prokázáno prostřednictvím experimentálních dat.
Klíčová slova: Otoakustické emise produktu zkreslení, PySide2, Synchronized Swept-Sine, Spodní hranice šumu, Analýza signálu..

1. Introduction

Swept sines are used to measure DPOAEs because they yield fast and reliable results with large frequency resolution [1][2]. Synchronized Swept-Sine (SSS) signals represent a distinctive class of signals characterized by exponential or logarithmic frequency sweeps [3]. Within this domain, the SSS technique emerges as a potent analytical tool, particularly relevant for nonlinear system analysis employing block-oriented models such as Generalized Hammerstein models and Diagonal Volterra Series [4].

DPOAEs are weak signals with level close to the level of background noise [5], necessitating repeated stimulus presentations and signal averaging to enhance their detectability [1][2]. In addition, DPOAEs are generally composed of two sources: (1) the primary source with nonlinear distortion as a generation mechanism and (2) the secondary source with linear reflection as a generation mechanism [6]. A recently presented technique of SSSs for DPOAE extraction allowed for reliable measurement and for separation of DPOAE components yielded by the two different sources[7]. The main aim of this thesis is to verify the presented SSS technique for DPOAE extraction for various sweep rates. Theoretically, the technique should be useable up to the sweep rate of 10 oct./sec for DPOAEs evoked with swept sines whose frequency ratio is about 1.2[8]. Here, we compare DP-grams (DPOAEs as a function of frequency for constant frequency ratio) for several sweep rates. Higher sweep rates lead to shorter signal duration, which should affect noise reduction by the method of averaging in time. Our second aim is to study how the sweep rate affect the background noise reduction during averaging in time. The findings presented in this thesis may enhance the accuracy and efficiency of DPOAE assessment, leading to improved diagnostic capabilities in audiology.

The Methods section of the thesis describes the SSS technique for DPOAE extraction. In addition, because in the development of interactive interfaces for DPOAE analysis; the

choice of technology plays a pivotal role in achieving a seamless and effective user experience the Methods section delves into the advantages of utilizing PySide2 for the creation of interactive interfaces. The Results section then shows recorded DP-grams. The obtained results are discussed in the Conclusion.

2. Methods

2.1 SSS in DPOAE

2.1.1 Benefits of SSSs in DPOAE measurement

In the realm of auditory research, particularly in the extraction of DPOAE from swept sine responses, several sophisticated techniques have been developed, each with its unique advantages and applications. One such method is the Least Squares Fitting Technique [12]. Another notable method is the Heterodyne Technique [13]. Additionally, Frequency Domain analysis, which involves transforming time-domain signals into the frequency domain, provides a comprehensive view of the frequency components present in the DPOAE response[9].

However, one of the hallmark advantages of the **synchronized swept sine technique** lies in its capacity to effectively disentangle frequency-dependent higher harmonics, rendering it invaluable for applications requiring harmonic separation. [4]

Of note is the adaptation of Novak's methodology [6] to the estimation of intermodulation DPOAEs, which themselves are a form of intermodulation distortion products. The inherent strength of the SSS technique is underpinned by its user-friendly implementation, computational efficiency, and the unique characteristic of being agnostic to the specific nonlinearity type within the system [2]. These attributes collectively position

the SSS technique as a promising instrument for incorporation into the realm of DPOAE measurements.

Intriguingly, the versatility of the SSS technique extends to the separation of DPOAE components characterized by varying latencies [2]. This capability amplifies its potential utility, as it addresses a critical aspect of DPOAE analysis. The confluence of features—ranging from harmonic separation and ease of implementation to its latency-discriminative ability—augments the allure of the SSS technique for enhancing the precision and insights attainable in DPOAE measurements.

In conclusion, the utilization of Specialized Synchronized Swept-Sine signals unveils an array of benefits that hold significant promise within the context of DPOAE investigations. By disentangling frequency-dependent harmonics and accommodating diverse nonlinearities, this technique emerges as a versatile and impactful tool for advancing our comprehension of auditory physiology.

2.1.2 Synchronized swept sines.

The theory behind SSS signals is described in Novak et al. [1]. Its application for DPOAE measurements is then described in Vencovsky et al. [2]. A SSS signal is a special case of an exponential swept sine defined as [1]

$$s(t) = \sin\big(\varphi(t)\big), \tag{1}$$

with the phase:

$$\varphi(t) = 2\pi f_a L exp\left(\frac{t}{L}\right). \tag{2}$$

The coefficient L related to the sweep rate is:

$$L = \frac{T}{\ln\left(\frac{f_b}{f_a}\right)}, \tag{3}$$

where f_a is the starting frequency and f_b is the stop frequency and T is the time duration of the signal. Multiplication of the phase $\varphi(t)$ by a positive integer m corresponds to the generation of the mth harmonic of the swept-sine, and is also equivalent to a time shift of the phase by Δt_m:

$$m\varphi(t) = \varphi(t - \Delta t_m), \tag{4}$$

$$\Delta t_m = -Lln(m). \tag{5}$$

Therefore, we can define a higher-harmonic version of the SSS as:

$$s_m(t) = \sin\big(m\varphi(t)\big) = \sin\big(\varphi(t - \Delta t_m)\big). \tag{6}$$

If we stimulate a nonlinear system with a pure tone, higher harmonics may appear at the output of the system. These higher harmonics are at frequencies of integer multiples of the pure tone frequency. The SSS technique allows for detection of these higher harmonics because those appear in the "virtual" impulse response yielded by

$$h(t) = F^{-1}\left\{\frac{Y(f)}{S(f)}\right\}, \tag{7}$$

$S(f)$ is the analytical equation for Fourier transform of the SSS; namely:

$$S(f) = \frac{1}{2}\sqrt{\frac{L}{f}}\exp\left\{j2\pi fL\left[1 - \ln\left(\frac{f}{f_a}\right)\right] - j\frac{\pi}{4}\right\}. \tag{8}$$

2.1.3 DPOAEs extracted with synchronized swept sines.

If we stimulate a nonlinear system with two pure tones, intermodulation distortion includes not only higher harmonics but also intermodulation products with frequency lower than the frequency of both tones. For example, $f_{m,n} = mf_1 + nf_2$, then for $m = 2$ and $n = 1$, the intermodulation product has a frequency $2f_1 - f_2$. This low side cubic difference tone is usually most salient intermodulation product for DPOAEs [3].

As with harmonic distortion, the SSS can be used to measure frequency-dependent intermodulation products using the property provided by Eq. (6). The input signal x(t) is a sum of two SSSs,

$$x(t) = \sin\left(\varphi_1(t)\right) + \sin\left(\varphi_2(t)\right), \tag{9}$$

with

$$\varphi_1(t) = 2\pi f_{1a} L exp\left(\frac{t}{L}\right), \tag{10}$$

$$\varphi_2(t) = 2\pi f_{2a} L exp\left(\frac{t}{L}\right). \tag{11}$$

The starting frequencies f_{1a} and f_{2a} of each synchronized swept sine are related by the coefficient $\alpha = \frac{f_{2a}}{f_{1a}} = \frac{f_{2b}}{f_{1b}}$. The coefficient L [Eq. (3)] is equal for the two SSSs, and is defined as

$$L = \frac{T}{\ln\left(\frac{f_{1b}}{f_{1a}}\right)} = \frac{T}{\ln\left(\frac{f_{2b}}{f_{2a}}\right)}, \tag{12}$$

f_{1b} and f_{2b} being, respectively, the stop frequencies of each swept-sine.

It is possible to generalize Eqs. (4), (5), and (6) [considering $\varphi(t) \equiv \varphi_1(t)$] as

$$(m + \alpha n)\varphi_1(t) = \varphi_1\left(t - \Delta t_{m,n}\right), \tag{13}$$

$$\Delta t_{m,n} = -L ln(m + \alpha n). \tag{14}$$

So

$$s_{m,n}(t) = \sin\left((m + \alpha n)\varphi_1(t)\right) = \sin\left(\varphi_1\left(t - \Delta t_{m,n}\right)\right). \tag{15}$$

for the f_1 tone at 0 time, which is useful because $f_{DP} = 2f_1 - f_2$ is adjacent to the f_1 component. This setting could be changed without any effect on the accuracy of the

technique [6].

Then the analytical equation for Fourier transform is given by:

$$S_1(f) = \frac{1}{2}\sqrt{\frac{L}{f}}\exp\left\{j2\pi fL\left[1 - \ln\left(\frac{f}{f_{1a}}\right)\right] - j\frac{\pi}{4}\right\}. \quad (16)$$

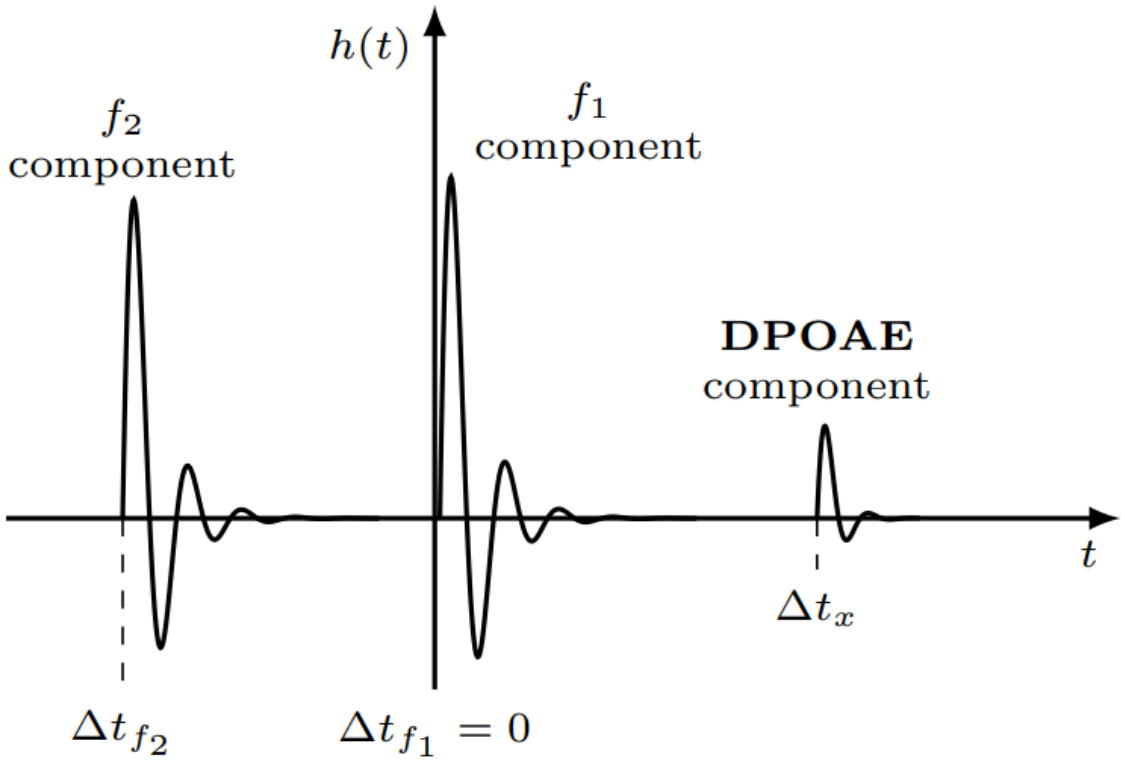

Fig.1 DPOAE

Figure 1 Demonstration of "virtual" impulse response for intermodulation distortion caused by a nonlinear system. The DPOAE component is at $2f_1 - f_2$.

Fig 1 demonstrates how the "virtual" impulse response $h(t)$ in case of intermodulation distortion looks. At t=0 and t=-delta t, we can see the impulse responses for the evoking stimuli f_1 and f_2, which are fed into the ear canal. The f_1 component is at time 0 because we used an analytical equation S_1 to calculate the "virtual" impulse response. The intermodulation distortion (DPOAE) at frequency $2f_1 - f_2$ is located at Δt time. Δt_{f_2} appears before f_1, indicating that the f_2 has higher frequency than the f_1

component. Δt_x is a pivotal parameter representing the time delay of the DPOAE component in relation to the primary frequency f_1 component. Fig 1 specifically addresses scenarios where the f_{DP} is defined as $2f_1 - f_2$, which typically resides below the f_1 tone in terms of frequency. The primary objective during DPOAE measurement is to accurately isolate and extract this DPOAE impulse response from the composite 'virtual' impulse response. By converting this component into the frequency domain, we can construct a DP-gram. This graph provides a detailed representation of the DPOAE amplitude and phase across varying frequencies, typically assessed at a constant $\frac{f_2}{f_1}$ ratio.

Furthermore, it is crucial to note that Fig 1 illustrates the virtual response for stimuli that are sequentially increased in frequency (where f_{1a} or f_{2a} are lower than f_{2a} or f_{2b}, respectively). In contrast, if the stimuli were to be decreased in frequency (a downward sweep), the resulting 'virtual' impulse response would display a reversed time axis. In such a scenario, while the f_1 component would maintain a time coordinate of zero, the DPOAE component would exhibit a negative time delay, and conversely, the f_2 component would present a positive time delay.

As we transition from understanding the virtual impulse responses to practical measurement considerations, it is imperative to acknowledge that the presence of noise can distort our perception and interpretation of the DPOAE signals. Thus, it is also important to analyze and reduce the noise within these measurements. This leads us to the necessity of employing temporal averaging techniques, detailed in the following subsection, to enhance the signal-to-noise ratio.

2.1.4 Temporal averaging technique for noise reduction

Because the DPOAE signal is weak, when measuring DPOAEs, it's crucial to consider and

analyze the noise present in the measurements. To reduce the noise, temporal averaging is performed. This means that response of the system is recorded repeatedly, and the recorded time-domain signals are averaged. This subsection describes how temporal averaging improves signal to noise ratio.

The RMS value is a measure of the "average" magnitude of a varying quantity over time. For a discrete signal $x[n]$ sampled over N points, the RMS value (P) is calculated as follows:

$$P = \sqrt{\frac{1}{N}\sum_{n=1}^{N}|x[n]|^2}. \tag{17}$$

$|x[n]|$ ensures that negative and positive values contribute equally to the average power. $|x[n]|^2$ squares each value, giving more weight to larger values. $\frac{1}{N}\sum_{n=1}^{N}|x[n]|^2$ calculates the average of the squared values. $\sqrt{\frac{1}{N}\sum_{n=1}^{N}|x[n]|^2}$ takes the square root to get the RMS value.

The decibel (dB) scale is a logarithmic scale commonly used in acoustics and signal processing. The formula to convert a pressure to sound pressure level in dB:

$$P_{dB} = 20log_{10}\left(\frac{P}{P_0}\right). \tag{18}$$

$p_0 = 2 \times 10^{-5}$ is the reference acoustic pressure in Pascals. $\frac{P}{P_0}$ calculates the ratio of the RMS value to the reference RMS value. $log_{10}\left(\frac{P}{P_0}\right)$ computes the logarithm base 10 of this ratio. $20log_{10}\left(\frac{P}{P_0}\right)$ scales the logarithmic value by 10 to convert it to decibels.

So, the result (L_{dB}) is the noise level in decibels relative to the reference sound pressure level. This approach is widely used in audio engineering and acoustics to quantify and compare signal levels. The reference pressure (P_0) was chosen to be close the hearing threshold at 1 kHz based on the sensitivity of the human ear, and 2×10^{-5} Pascals is a common reference for sound pressure level measurements in air.

```python
import numpy as np
import matplotlib.pyplot as plt

# Sets the length of each random noise signal to be 2^12 samples.
N = 2 ** 12
# Initializes the accumulated signal to zero.
Ssig = 0
# Creates an array to store the RMS values over 30 repetitions.
RMSvalue = np.zeros(30, )
for i in range(30):
    # Generates a random noise signal.
    signal = np.random.randn(N)
    Ssig += signal
    RMSvalue[i] = np.sqrt(np.mean(Ssig ** 2))
# Plots the logarithmic decrease in RMS values over repetitions.
fig, ax = plt.subplots()
ax.plot(20 * np.log10(RMSvalue / np.arange(1, 30 + 1)))
plt.title("Noise Level Decay with Repetitions", fontsize=25)
plt.xlabel('Repetitions', fontsize=25)
plt.ylabel('Noise level (dB SPL)', fontsize=25)
plt.tick_params(labelsize=20)
plt.show()
```

Fig.2 Python code for noise analysis.

The code in Fig.2 generates random noise signals, accumulates them, calculates the root mean square (RMS) value at each accumulation step, and then plots the logarithmic decrease in RMS over the repetitions.

In case of DPOAE measurements, we record a signal which should be stable over time because we assume that the system is time-invariant. If we assume that the noise is normally distributed and independent in each recoding, summing the N responses should lead to linear growth in the RMS value of the signal but square-root growth in the RMS value of the noise. Here we provide a simulation showing the noise level during temporal averaging.

This code simulates the generation of random noise signals using a pseudo-random

number generator that outputs values with a standard normal distribution (mean of zero and variance of one). The length of each noise signal is set to 2^12 samples, which may represent a specific time window in actual signal processing scenarios. An accumulated signal is constructed by summing up 30 instances of these random signals, which is then used to calculate the RMS level of the accumulated signal.

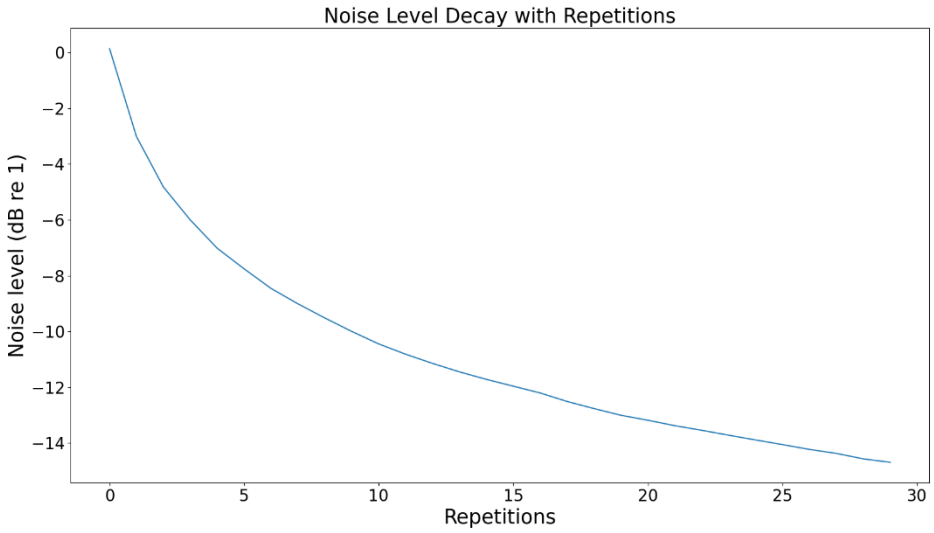

Fig.3 Logarithmic Decrease of Noise Level Across Repetitions

As shown in Fig.3, after the above processing, we can clearly see the noise level decreases over time.

2.2 Software tools

Within the scope of developing a user interface for DPOAE measurement analysis, a strategic decision was made to adopt PySide2 as the foundational technology. This choice was informed by a comprehensive evaluation of potential tools, with a specific focus on the comparative benefits PySide2 provides over other technologies, such as MATLAB, for this application.

The selection of PySide2 is justified by several key factors. Firstly, its exceptional capacity for easy integration with Python allows for the seamless inclusion of custom DPOAE analysis algorithms, ensuring a smooth and user-friendly experience. Additionally,

PySide2's compatibility with Python leverages the language's powerful, succinct syntax and rich library ecosystem, making it an ideal match for scientific computing needs. Another significant advantage is the robust support provided by the PySide2 community: a dynamic and resource-rich network offering documentation and collaborative opportunities that are crucial for rapid and innovative interface development.

2.2.1 Pyside2 interface

Initially, the development of our interactive interface commenced with the utilization of Qt Designer, a renowned tool for designing GUIs, which allowed for the meticulous crafting of a user-friendly interface. The subsequent implementation phase involved Python and the PySide2 library, a combination chosen for its robustness and flexibility. During the programming process, we strategically employed a multithreading approach, an essential technique for managing multiple concurrent operations within the application.

Multithreading was pivotal for our interface, considering the real-time nature of DPOAE measurements. It is not a trivial implementation; rather, it necessitates a sophisticated understanding of concurrent programming paradigms. By utilizing two threads, we could decouple the measurement process from the user interface. The main thread is dedicated to the UI, ensuring that it remains responsive and capable of receiving user input without lag, which is critical for maintaining an interactive experience. Any delay or unresponsiveness in the UI could lead to errors in parameter entry or misinterpretation of the results, compromising the accuracy of the DPOAE measurements.

In parallel, the secondary thread works diligently in the background, handling the intensive task of processing DPOAE measurements. The thread must handle real-time data acquisition and processing, which is computationally demanding and could lead to significant performance bottlenecks if executed on the main thread.

This multithreaded design is far from straightforward due to the complexities involved in ensuring thread safety and avoiding race conditions where two threads attempt to access the same resources simultaneously. Careful synchronization mechanisms are implemented to prevent such conflicts, ensuring data integrity and reliable operation of the measurement process. By adopting this sophisticated multithreading approach, our interface can simultaneously handle user interactions and complex data processing tasks.

```
from PySide2.QtUiTools import QUiLoader
from PySide2.QtCore import *
from PySide2.QtWidgets import *
from PySide2.QtGui import *
from UserModules.pyDPOAEmodule import *
import time
from scipy.io import savemat
import datetime
from UserModules.pyRMEsd import *  # import needed functions from pyRMEsd module
import matplotlib
from UserModules.draw import *
from matplotlib.backends.backend_qt5agg import FigureCanvasQTAgg as FigureCanvas
from matplotlib.figure import Figure
import os
```

Fig.4. Importing the required modules

```
def get_time() -> str:
    # to get current time
    now_time = datetime.datetime.now().strftime('%Y_%m_%d_%H_%M_%S')
    return now_time
```

Fig.5. The function get_time() that returns the current time as a string.

The code is a PySide-based application for running a DPOAE simulation and displaying the results graphically. It includes various import statements and a class Worker that manages the simulation in a separate thread.

```
class Worker(QThread):
    """Object managing the simulation"""

    stepIncreased = Signal(int)

    graph_generated = Signal(Figure)

    def __init__(self, ui):
        super().__init__()
```

Fig.6. The class Worker

The Worker inherits from QThread and handles the simulation. It includes various member variables and methods such as run(), generate_graph(), and chirps().

```
233 class SimulationUi(QWidget):
234     """main thread"""
235 
236     def __init__(self, widget_choose):
237         super().__init__()
```

Fig.7. Class SimulationUi.

The SimulationUi inherits from QWidget and represents the main application window. It includes methods for handling user interactions and displaying the graph.

The above codes can be found from: [14]

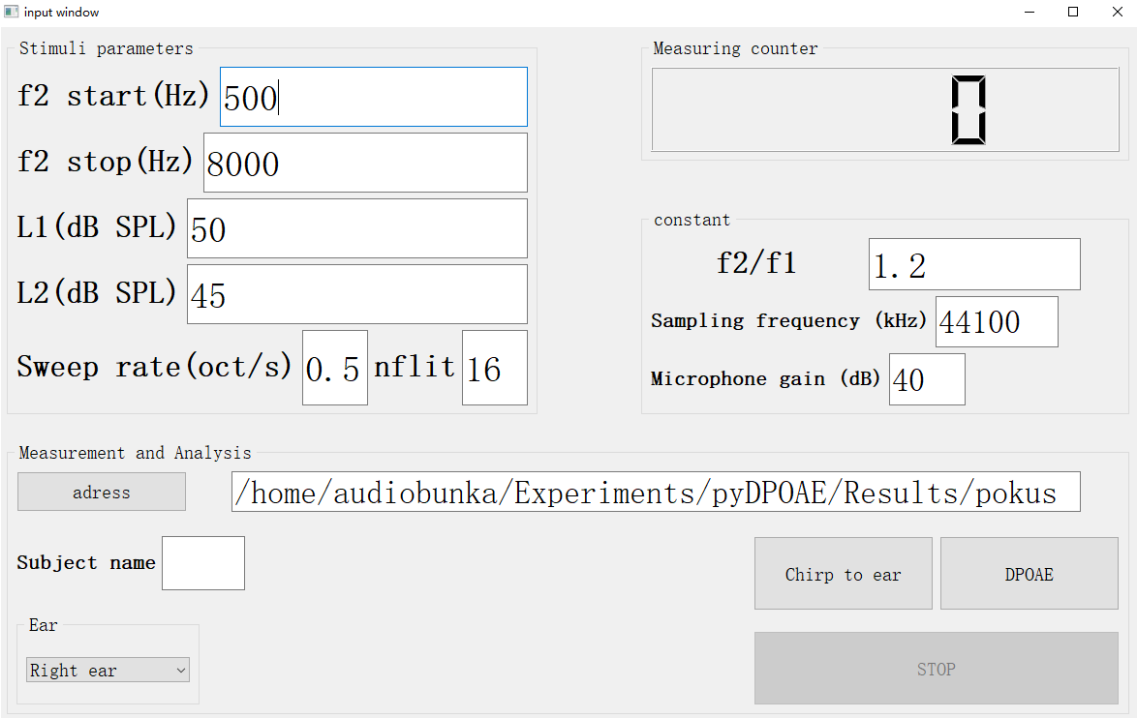

Fig.8. Interactive interface display.

2.3 Data acquisition

DPOAEs were measured with SSSs of various stimulus levels ($L_1 = 60$ dB SPL, and $L_2 =$

50 dB SPL,, or $L_1 = 50$ dB SPL, and $L_2 = 45$ dB SPL), the frequency ratio between the stimuli $\frac{f_2}{f_1} = 1.2$, and f_2 tone swept at a rate of 0.5 oct/s, 1 oct/s, 2 oct/s 4 oct/s 8 oct/s. between 500Hz and 8 kHz. The onset and offset of the swept-sines were shaped with 20-ms long raised-cosine ramps. All measurements were done in an audiological booth using custom software written in PYTHON. Sound signals were generated in a computer and were presented by an ETYMOTIC RESEARCH OAE probe (ER-10C DPOAE PROBE DRIVER-PREAMP) connected to a sound card RME Fire face UCX. For the communication with sound card, we used the sound device library[11]. The measurements were done with sampling frequency of 44.1 kHz. In order to present the sound signal into the ear canal with the correct sound pressure level, the probe has to be calibrated. We used an in-situ calibration technique and calibrated the probe after it was placed into the ear canal. To measure the transfer function of the probe in the ear canal, we used repeatedly presented chirps linearly swept between 0 and 22.05 kHz across 2048 samples. We presented the chirps 300 times over each speaker and averaged the resulting response.

As mentioned above, stimuli were delivered into the ear canal multiple times to diminish the noise floor (NF), a critical step in enhancing the clarity of the resultant DP-gram. To accurately assess and manage this noise, a noise matrix is created for each repetition of the stimuli. This matrix is instrumental in identifying and quantifying noise elements inherent in each measurement. Following this, the noise floor is estimated from the averaged noise signal by employing the same SSS technique used for DPOAE measurements. This method ensures a consistent and accurate representation of the noise floor. The iterative process of stimulus presentation and DP-gram computation allows the experimenter to terminate the measurement procedure once a reliable decision can be made about the stability of the recorded data. Specifically, the measurement is concluded when both the DP-gram and the associated background noise exhibit negligible variation, ensuring the reliability and clarity of the obtained results. In addition, we selected the noise to be between $2f_1 - f_2$ and $3f_1 - 2f_2$ f_{DP}

component. The noise data obtained in this way reduces the influence of the impulse response in the test and the influence of the movement, swallowing and other behaviors of the subject.

One of the salient benefits of employing the SSS technique in this research is its computational efficiency. This advantage is particularly noteworthy as it enables the real-time calculation of the DP-gram concurrent with the measurement process. Such computational expediency not only facilitates immediate data analysis but also significantly streamlines the experimental procedure. The methodologies and procedures have been rigorously executed in strict adherence to the guidelines and protocols delineated in paper [7].

Furthermore, the system is designed to archive all raw recordings, thereby allowing for subsequent post-hoc analysis using alternative DPOAE extraction methods. This archival feature ensures that data is not solely analyzed in situ but can also be re-examined in the future to potentially uncover additional insights.

Fig.9 ETYMOTIC RESEARCH ER10C probe preamplifier

In this project, the participant group was selected to consist of adults aged 20 to 30, a demographic typically associated with stable hearing capabilities. The majority of these

participants are male international students, offering a sample with varied cultural backgrounds but uniform in terms of auditory health. All individuals were pre-screened to confirm normal hearing levels, aligning with the study's requirements for standard baseline auditory function.

3. Results

This section contains two subsections, the first shows the effect of sweep rate on DP-grams and the other one study how the noise floor changes for various sweep rates with the number of repetitions.

3.1 Effect of sweep rate on DP-grams

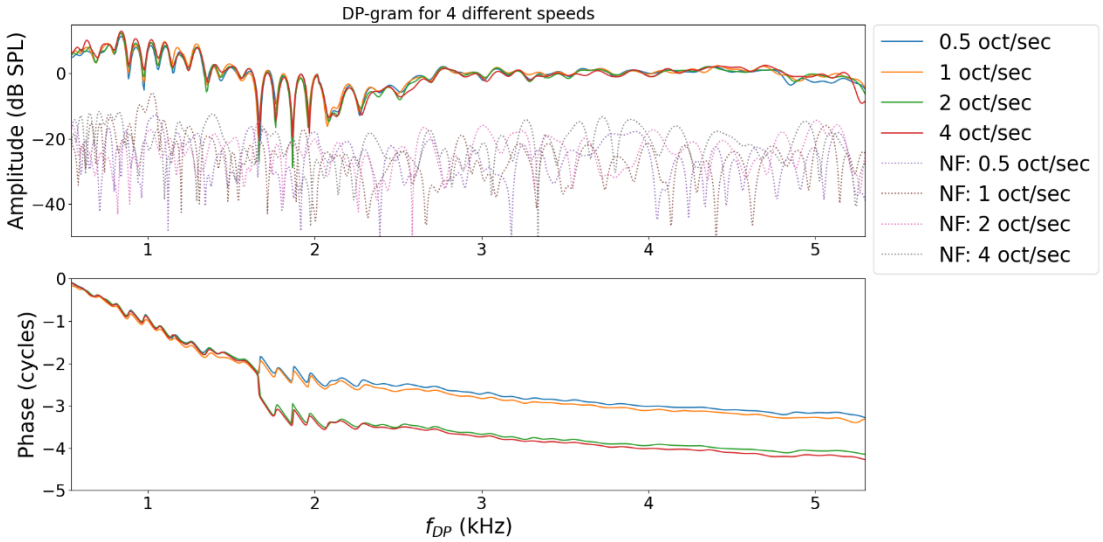

Fig.10 Amplitude and phase plots of DP-gram from subject s039 for different speeds of sweeping.

Fig.10 shows amplitude and phase of the DP-gram measured in subject s039 (right ear) for various sweep rates indicated in the legend. The solid lines depict DP-grams derived

by the SSS technique and the dotted lines depict estimated noise floors. The swept sine parameters are: $L_1 = 50dB\ SPL$, $L_2 = 45dB\ SPL$, the initial f_2 frequency is $500Hz$ and the final f_2 frequency is $8kHz$, which for $\frac{f_2}{f_1}$ is 1.2 yields the f_{DP} frequency range of about $0.54kHz$ and $5.3kHz$. The DP-grams were calculated by averaging the SSS responses for 21 repetitions for 0.5 oct/sec, 39 repetitions for 1 oct/sec, 45 repetitions for 2 oct/sec, 62 repetitions for 4 oct/sec.

Figure 11 then depicts the DP-gram from Fig. 10 in narrow frequency range to visualize possible sweep rate effects on DP-gram amplitude fine structure.

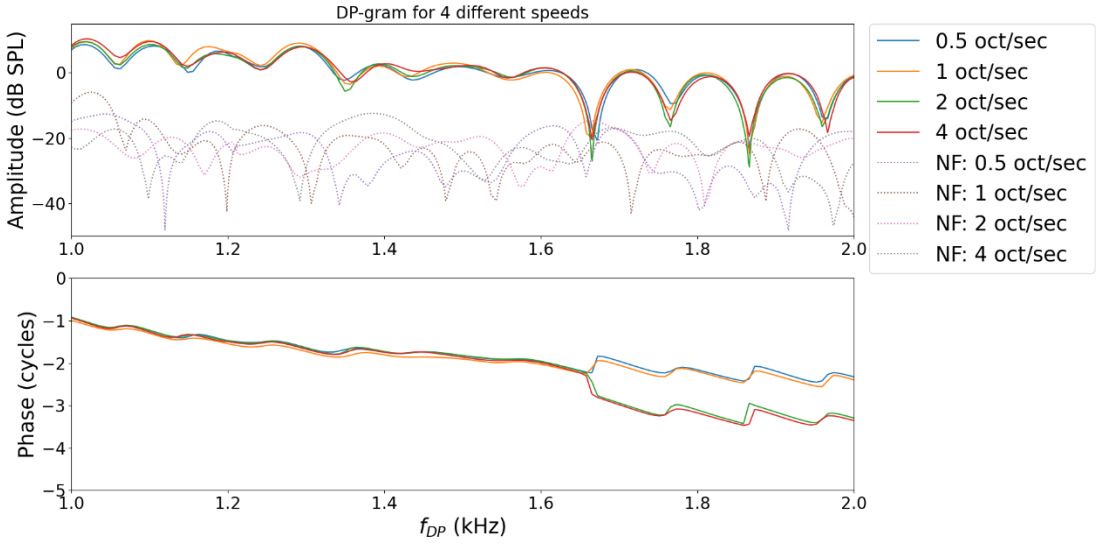

Fig.11 The same data as in Fig.10. with x-axis ranging from 1 to 2 kHz.

According to Fig.11, we can see there is no systematic shift in the fine structure of DP-gram amplitude with sweep rate. It can be preliminarily concluded that the DP-gram is roughly the same at four different frequency sweep speeds. The visible changes between each measurement are most probably due to the measurement inaccuracy caused by background noise and measurement artifacts (e.g., subject movement, breathing etc.).

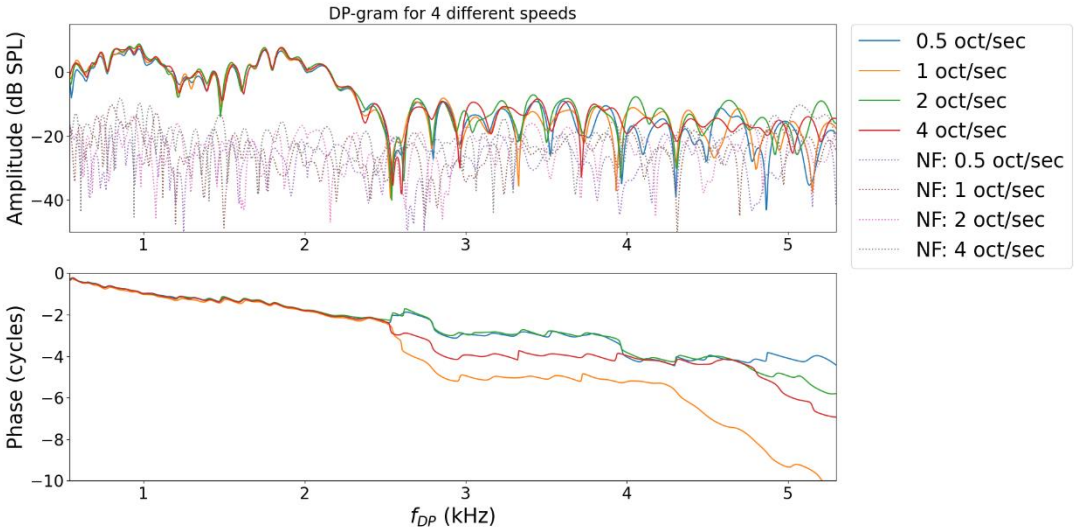

Fig.12 Amplitude and phase of a DP-gram for subject s050

Figure.12 shows amplitude and phase of the DP-gram measured in subject s050 (right ear) for various sweep rates indicated in the legend. The solid lines depict DP-grams derived by the SSS technique and the dotted lines depict estimated noise floors. The swept sine parameters are: $L_1 = 50dB\ SPL$, $L_2 = 45dB\ SPL$, the initial f_2 frequency is $500Hz$ and the final f_2 frequency is $8kHz$, which for $\frac{f_2}{f_1}$ is 1.2 yields the f_{DP} frequency range of about $0.54kHz$ and $5.3kHz$. The DP-grams were calculated by averaging the SSS responses for 21 repetitions for 0.5 oct/sec, 34 repetitions for 1 oct/sec, 43 repetitions for 2 oct/sec, 59 repetitions for 4 oct/sec.

Figure.13 then depicts the DP-gram from Fig.12 in narrow frequency range to visualize possible sweep rate effects on DP-gram amplitude fine structure.

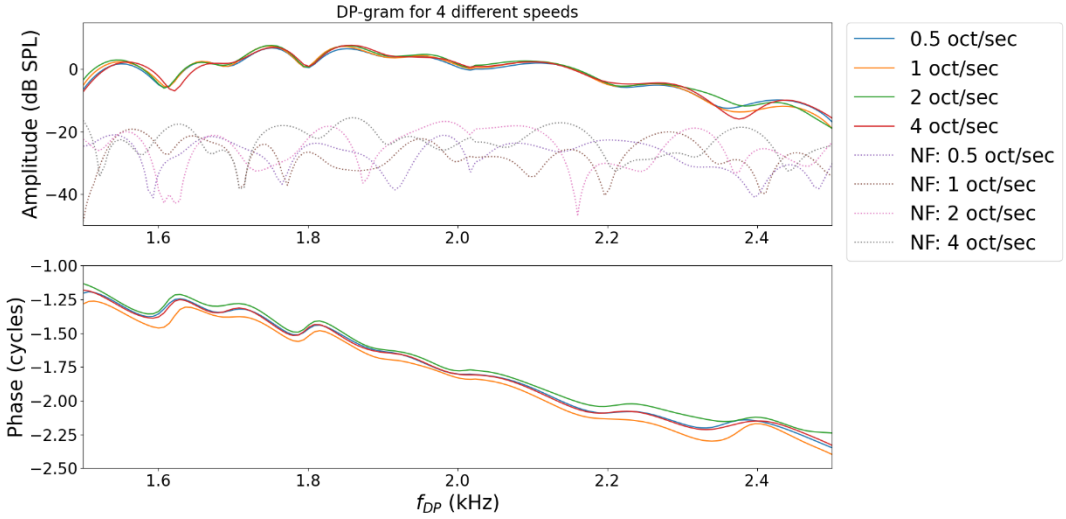

Fig.13 the same data as in Fig.12. with x-axis ranging from 1.5 to 2.5 kHz.

Just visually inspecting Fig.13, we can make the same conclusion as above that the sweep rate does not cause any systematic shift in the fine structure of DP-gram amplitude. The visible changes between each measurement are most probably due to the measurement inaccuracy caused by background noise and measurement from Fig.10 and Fig.11 in the previous article.

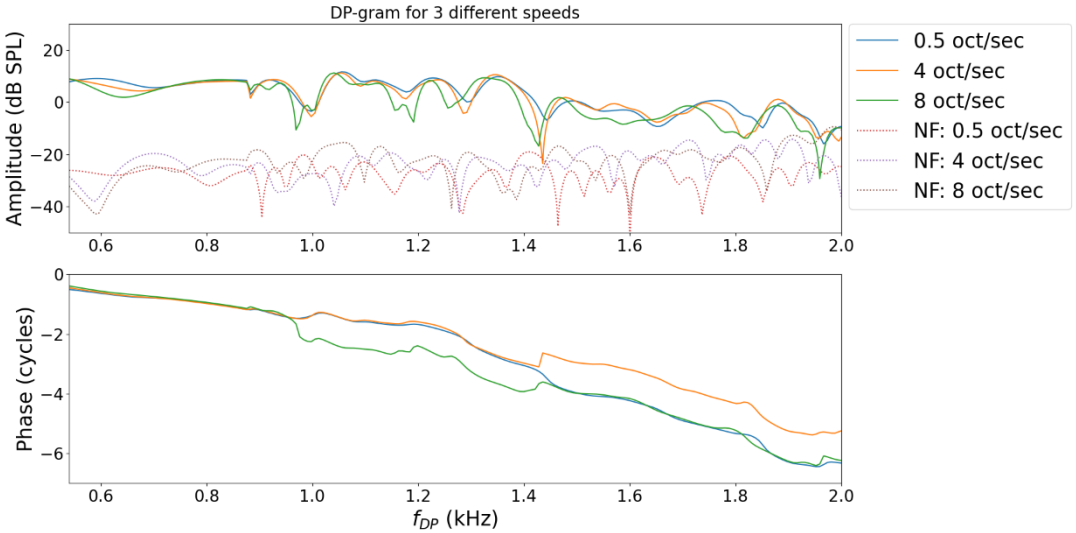

Fig.14 Amplitude and phase of a DP-gram for subject s051

Figure.14 shows amplitude and phase of the DP-gram measured in subject s051 (right ear) for various sweep rates indicated in the legend. The solid lines depict DP-grams derived by the SSS technique and the dotted lines depict estimated noise floors. The swept sine parameters are: $L_1 = 50dB\ SPL$, $L_2 = 45dB\ SPL$, the initial f_2 frequency is $8kHz$ and the final f_2 frequency is $500Hz$, which for $\frac{f_2}{f_1}$ is 1.2 yields the f_{DP} frequency range of about $0.54kHz$ and $5.3kHz$. The DP-grams were calculated by averaging the SSS responses for 20 repetitions for 0.5 oct/sec, 50 repetitions for 4 oct/sec, 72 repetitions for 8 oct/sec.

Amplitude fine structure of the DP-gram in Fig. 14 for 8 oct/sec departs most from the other two sweep rates (0.5 and 4 oct/sec.). For this stimulus setup and measurement paradigm, we are probably approaching a speed limit for which we can use the SSS technique using upward sweeps. This indicates that the theoretical limit of 10 oct/sec for the sweep rate in the SSS technique given in [7] is probably too large and the real limit is lower (< 8 oct/sec). If we want to be conservative, we can suggest that 4 oct/sec sweep rate could be optimal in this frequency range (f2=500 to 8000 Hz) and for this frequency ratio (1.2).

In all free subjects and sweep rates (Fig. 10-14), we concluded the DP-gram's fine structure was stable across different sweep rates and that we did not observe any systematic shifts in the fine structure. This stability is crucial as it implies that DPOAE measurements can be reliably conducted at various sweeping speeds without significant loss of data integrity. At the same time, this result contrast with the sweep-rate and direction effect on DP-gram fine structure presented [8]. That study showed the effect of sweep rate and direction of sweeping (upward vs downward sweeps) on shifts in DP-gram fine structure. They showed a systematic shift. However, the paper [9] showed that the sweep rate and direction effect shown in [8] was due to the method of least-square

fitting which was used by the authors to extract the DP-grams form the swept sine responses. Our current results prove the explanation given in the paper [9]. In addition, this thesis shows that the SSS technique is free of such a systematic error present in the least-square fitting technique. It should be also noted that the SSS technique used in this thesis allowed for the use of much higher sweep rates (4 and even 8 oct/sec) than in the studies [8] and [9] (maximally 2 oct/sec).

However, higher sweep rate may be useless if it requires larger number of repetitions [2]. Therefore, in next subsection, we study how the estimated noise floor changes with repeated recordings of swept sine responses.

3.2 Noise analysis

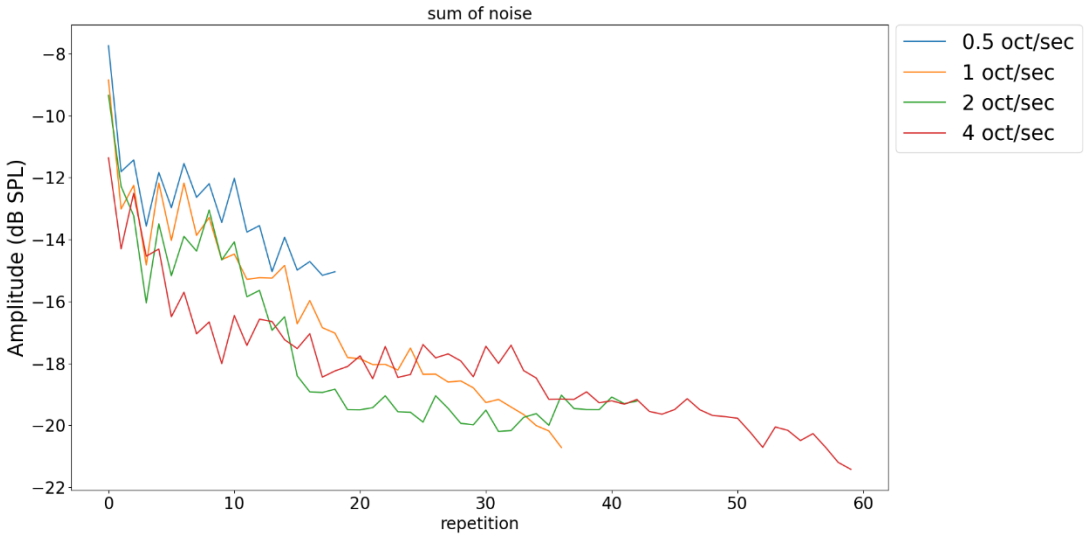

Fig.15 Sum of noise level for subject s039 following Fig.10

In Figure 15, a systematic analysis reveals a notable trend: as the number of repetitions increases, there is a consistent decrease in noise levels. This observation holds true across different sweep rates. Specifically, for a sweep rate of 2 oct/sec, the noise level tends to stabilize after approximately 20 repetitions. Interestingly, even when the sweep rate is increased to 4 oct/sec, a similar pattern of decline in noise level is observed, with stabilization occurring around 50 repetitions. This similarity in noise reduction across

different sweep rates suggests that increasing the sweep rate up to 4 oct/sec may not necessitate a proportional increase in the number of measurements. It's important to note, however, that the final outcome can be influenced by subject behavior. For instance, at higher sweep rates, physiological responses such as swallowing could significantly affect parts of the response. In our measurement, we used artifact rejection method following paper [7]. However, for the threshold θ, instead $\theta = 2\sigma$, we used $\theta = 10\sigma$ because the small θ yielded worse result. Nevertheless, the benefits of using higher sweep rates, particularly in terms of efficiency and potential for improved data quality, appear to be promising and warrant further investigation.

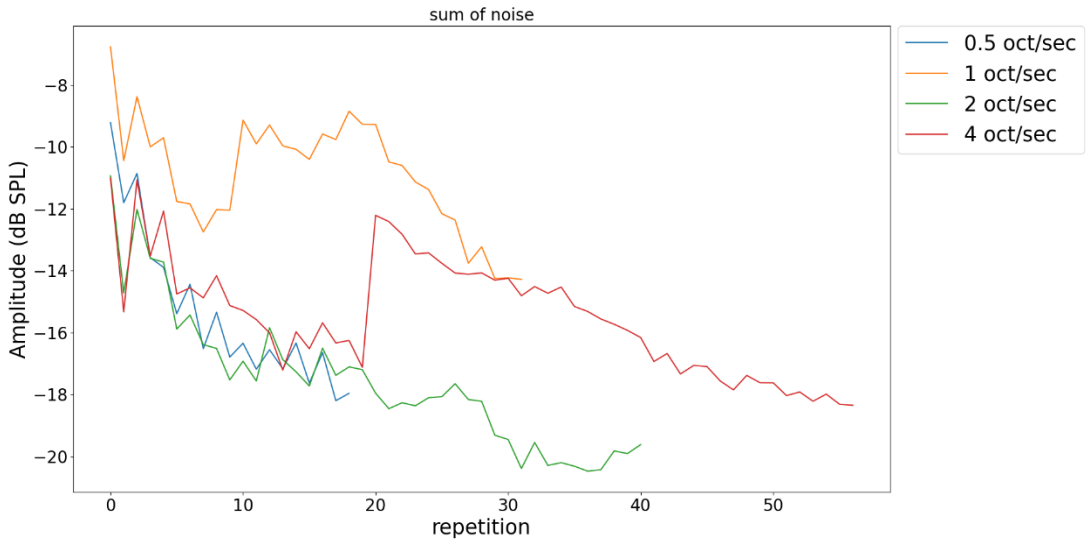

Fig.16 Sum of noise level for subject s050 following Fig.12

In Figure 15 and 16, systematic analyses reveal a consistent trend: as the number of repetitions increases, there is a notable decrease in noise levels across various sweep rates. For sweep rates of 0.5 and 2 oct/sec, the noise level tends to stabilize after approximately 20 repetitions, indicating a threshold beyond which further repetitions do not significantly enhance signal clarity. However, an intriguing phenomenon is observed at 1 oct/sec and 4 oct/sec sweep rates, where the noise level unexpectedly rises after initially decreasing. After this rise, the data continue to exhibit a downward trend in noise levels. The reason may come from unknown reasons such as the movement or swallowing of the subject. Since then, data have shown a continued downward trend.

4. Conclusion

This thesis embarked on a detailed exploration of the impact of swept-sine speed on the characteristics of DPOAE. The study was primarily focused on how different sweep rates influence the DP-grams and the associated noise levels in DPOAE measurements.

Our investigations revealed that the fine structure of DP-grams remains stable across various sweep rates. Significantly, we observed that this stability extends up to a sweep rate of 4 octaves per second. This finding is crucial as it suggests that DP-grams could be measured with faster sweeps than traditionally used (less than 2oct/sec), potentially enhancing the efficiency of DPOAE testing without compromising the quality and reliability of the results.

In addition, we also delved into the analysis of noise levels in DPOAE measurements across different sweep rates. We found that the noise interference is similar at different sweep rates. Noise levels tend to decrease with increasing sweep repetitions. This result further indicates that the SSS technique can be used to fasten DPOAE measurement. Therefore, the technique seems to be promising for diagnostic purposes.

For the future work, we would suggest to vary the phase of the stimuli in the way which leaves on the f_{DP} tone at $2f_1 - f_2$ and cancels the evoking tones and their higher harmonics and other distortion products like suggested in the paper [10]. Our pilot experiment indicated that with this phase ensemble, we can achieve even larger sweep rate than 8 oct/sec used in this thesis.

Bibliography and references

[1] Long GR, Talmadge CL, Lee J. Measuring distortion product otoacoustic emissions using continuously sweeping primaries. J Acoust Soc Am. 2008 Sep;124(3):1613-1626. doi: 10.1121/1.2949505. PMID: 19045653.

[2] Abdala C, Luo P, Shera CA. Optimizing swept-tone protocols for recording distortion-product otoacoustic emissions in adults and newborns. J Acoust Soc Am. 2015 Dec;138(6):3785-3799. doi: 10.1121/1.4937611. PMID: 26723333; PMCID: PMC4691260.

[3] Novak A, Simon L, Lotton P. Synchronized Swept-Sine: Theory, Application, and Implementation. Journal of the Audio Engineering Society, 2015, 63 (10), pp.786-798. ⟨10.17743/jaes.2015.0071⟩. ⟨hal-02504321⟩

[4] Novak A, Simon L, Kadlec F and Lotton P. "Nonlinear System Identification Using Exponential Swept-Sine Signal," in IEEE Transactions on Instrumentation and Measurement, vol. 59, no. 8, pp. 2220-2229, Aug. 2010, doi: 10.1109/TIM.2009.2031836.

[5] Probst R, Lonsbury-Martin BL, Martin GK. A review of otoacoustic emissions. J Acoust Soc Am. 1991 May;89(5):2027-2067. doi: 10.1121/1.400897. PMID: 1860995.

[6] Christopher A. Shera, John J. Guinan; Evoked otoacoustic emissions arise by two fundamentally different mechanisms: A taxonomy for mammalian OAEs. J Acoust Soc Am 1 February 1999; 105 (2): 782–798.

[7] Vencovský V, Novak A, Klimeš O, Honzík P, Vetešník A. Distortion-product otoacoustic emissions measured using synchronized swept-sines. J Acoust Soc Am 1 May 2023; 153 (5): 2586–2599.

[8] AlMakadma HA, Henin S, Prieve BA, Dyab WM, Long GR. Frequency-change in DPOAE evoked by 1 s/octave sweeping primaries in newborns and adults. Hear Res. 2015 Oct; 328:157-165. doi: 10.1016/j.heares.2015.08.012. Epub 2015 Aug 28. PMID: 26318364.

[9] Shera CA, Abdala C. Frequency shifts in distortion-product otoacoustic emissions evoked by swept tones. J Acoust Soc Am. 2016 Aug;140(2):936. doi: 10.1121/1.4960592. PMID: 27586726; PMCID: PMC5392090.

[10] Whitehead ML, Stagner BB, Martin GK, Lonsbury-Martin BL. Visualization of the onset of distortion-product otoacoustic emissions, and measurement of their latency. J Acoust Soc Am. 1996 Sep;100(3):1663-1679. doi: 10.1121/1.416065. PMID:

8817893

[11] https://python-sounddevice.readthedocs.io/en/0.4.6/

[12] Long GR, Talmadge CL, Lee J; Measuring distortion product otoacoustic emissions using continuously sweeping primaries. J. Acoust. Soc. Am. 1 September 2008; 124 (3): 1613–1626.

[13] Choi YS, Lee SY, Parham K, Neely ST, Kim DO. Stimulus-frequency otoacoustic emission: measurements in humans and simulations with an active cochlear model. J Acoust Soc Am. 2008 May;123(5):2651-2669. doi: 10.1121/1.2902184. PMID: 18529185; PMCID: PMC2481564..

[14] https://github.com/vencov/pyDPOAE